Mitotane activates ATF4/ATF3 axis triggering endoplasmic reticulum stress in adrenocortical carcinoma cells

Biomedicine & Pharmacotherapy 184 (2025) 117917

Contents lists available at ScienceDirect

Biomedicine & Pharmacotherapy

journal homepage: www.elsevier.com/locate/biopha

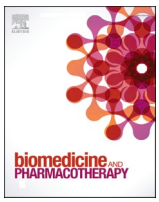

Mitotane activates ATF4/ATF3 axis triggering endoplasmic reticulum stress in adrenocortical carcinoma cells

Aurora Schiavon [a], Laura Saba [a], Carlotta Evaristo [a], Jessica Petiti [b,*], Ymera Pignochino [a,c], Giulio Ferrero [a], Giorgia Giordano [c,d], Cristina Tucciarello [a,c], Soraya Puglisi [a], Giuseppe Reimondo [a], Massimo Terzolo [a,1], Marco Lo Iacono [a,*,1]

[a] Department of Clinical and Biological Sciences, University of Turin, Turin, Italy
[b] Division of Advanced Materials Metrology and Life Sciences, Istituto Nazionale di Ricerca Metrologica (INRiM), Turin, Italy
[c] Candiolo Cancer Institute, FPO-IRCCS, Candiolo, Turin, Italy
[d] Department of Oncology, University of Turin, Turin, Italy

ARTICLE INFO

Keywords:
Adrenocortical carcinoma
Mitotane
RNAseq
ATF4
ATF3
ER stress

ABSTRACT

Adrenocortical Carcinoma is a rare and aggressive endocrine malignancy, that arises from cells of one of the three cortical layers of the adrenal gland. Radical surgery is the only curative treatment, even if recurrence rates are high. Therapeutic options are limited, with mitotane as the cornerstone of medical therapy. Despite 50 years of clinical use, the mechanism of action of mitotane has not yet been fully established, possibly due to the drug's susceptibility to interaction with confounding factors that reduce its biological activity. In the present study, we evaluated by RNAseq the effect of mitotane on gene expression in the H295R cell line, in an environment free of known confounding factors. Our approach allowed us to identify transcriptional deregulation of the ATF4/ATF3 axis, often involved in ER stress. These results were also validated by ddPCR in independent experiments. Mitotane-mediated ATF4 overexpression was also confirmed at the protein level. We observed how an incremental concentration of mitotane could deregulate main biological pathways. Further, we confirmed, both at RNAseq and ddPCR level, the mitotane-mediated downmodulation of genes such as *STAR*, *CYP11A1*, *CYP21A2*, and *HSD3B2*, highlighting its effect on steroid hormones biosynthesis. Through our approach, we identified biological pathways altered by mitotane in early response stages and with low drug concentrations. Some of these pathways could potentially be investigated in the future as functional biomarkers to monitor adrenocortical carcinoma treatment or as new pharmacological targets for this rare disease.

1. Introduction

Adrenocortical Carcinoma (ACC) is a rare and aggressive endocrine malignancy, with an estimated incidence of 0.5–2 new cases per million people per year [1] and an overall 5-year survival rate between 16 % and 47 %, highlighting the poor prognosis associated with this cancer [2–4]. ACC is usually sporadic, but it has a congenital (Beckwith-Wiedemann syndrome) and/or hereditary (Li-Fraumeni syndrome, MEN1, Gardner syndrome, Lynch syndrome) form [5]. ACC arises from cells of one of the three cortical layers of the adrenal gland and frequently causes an increase in steroid hormone production. About 50 %-60 % of patients show clinical manifestations of steroid excess, such as Cushing's Syndrome, virilization, and Conn's syndrome; frequently, mixed phenotypes are evident given that multiple steroids may be concomitantly secreted by the tumor [4,6–9]. The driver genes underlying the differences between ACC and other types of adrenocortical tumors remain unknown [10]. Significant insight into ACC biology has been provided by the comprehensive pan-molecular characterizations of many ACC cases performed by the two consortia, ENS@T [11] and TCGA [12].

Up to now, a limited range of therapeutic options is available for ACC

* Corresponding authors.
E-mail addresses: aurora.schiavon@unito.it (A. Schiavon), laura.saba@unito.it (L. Saba), carlotta.evaristo@unito.it (C. Evaristo), j.petiti@inrim.it (J. Petiti), ymera.pignochino@unito.it (Y. Pignochino), giulio.ferrero@unito.it (G. Ferrero), giorgia.giordano@unito.it (G. Giordano), cristina.tucciarello@unito.it (C. Tucciarello), soraya.puglisi@unito.it (S. Puglisi), giuseppe.reimondo@unito.it (G. Reimondo), massimo.terzolo@unito.it (M. Terzolo), marco.loiacono@unito.it (M. Lo Iacono).
[1] M.L. and M.T. equally contributed to this manuscript.

https://doi.org/10.1016/j.biopha.2025.117917
Received 11 December 2024; Received in revised form 8 February 2025; Accepted 14 February 2025
Available online 17 February 2025

patients, with radical surgery remaining the only curative treatment, even though recurrence is reported in up to 60 %-70 % of patients [4,13–15]. Mitotane remains the cornerstone of medical therapy used either as monotherapy or in combination with classical cytostatic agents [16–18]. Mitotane is also increasingly used in the postoperative adjuvant setting [19]. Mitotane, also known as 1,1-(o,p-Dichlorodiphenyl)-2, 2-dichloroethane (o,p'-DDD), commercially marketed under the brand name Lysodren® (HRA Pharma Rare Diseases, Paris, France), is derivative of the insecticide DDT, from which it was first isolated in 1940, and approved by the Food and Drug Administration in 1970 for ACC treatment [20,21]. Mitotane primarily exerts its pharmacological effects on the adrenal cortex, particularly in the *zona fasciculata* and *zona reticularis,* leading to cell damage and impairment of the steroidogenesis process [22].

Despite years of use in the clinic, the mechanism of action is still unclear. The pharmacological effect of mitotane is thought to depend on the inhibition of steroidogenesis, intracellular lipid accumulation, and endoplasmic reticulum (ER) stress induction, leading to cell death [23]. Mitotane has a massive effect on steroidogenesis, although it remains unclear whether it inhibits key enzymes (e.g., CYP11A1 or CYP11A2), steroidogenic regulatory genes (e.g., *SREBF* coding for the Sterol Regulatory Element-Binding Transcription Factor) or both [24]. The inhibition of SOAT1 (Sterol-O-acyl transferase 1) and the deriving ER stress are possible key molecular pathways activated by mitotane [25]. Studies showed that mitotane-mediated apoptosis and necroptosis may also be induced by the blockage of mitochondrial respiratory chain complexes I and IV, as well as the disassembly of mitochondria-associated membranes [26,27].

A possible reason for our limited understanding of the mitotane mechanism of action is the high susceptibility of *in vitro* experiments to the presence of confounding factors. Intriguingly, mitotane cytotoxicity seems to vary between experiments from different research groups, even when carried out on the same cell lines [23]. In fact, in our previous work, we demonstrated that the presence of confounding factors in culture media (such as BSA, commercial serum, and patient serum) interferes with the pharmacological effect of mitotane [28]. Similar results have been observed in other studies by Hescot et al., in which they identified an inverse correlation between mitotane activity and lipoprotein concentration in the media [29].

Considering these data, mitotane resistance could be an artifact caused by the experimental conditions, resulting in an inaccurate evaluation of the mitotane pharmacological effect. In this study, we aimed to evaluate the mitotane effect on gene expression and the regulation of biological pathways under experimental conditions free of known confounding factors.

2. Materials and methods

2.1. Drugs and chemicals

Mitotane was dissolved in absolute ethanol in a 156 mM stock solution and stored at −20°C. The drug was provided by MedChemExpress LLC (Monmouth Junction, NJ 08852, USA).

2.2. Cell lines and culture conditions

H295R cells were kindly provided by Prof. S. Sigala (Department of Molecular and Translational Medicine, University of Brescia, 25123 Brescia, Italy) and cultured at 37°C with 5 % CO_2 according to American Type Culture Collection (ATCC) instructions. Media and supplements were purchased from Euroclone. H295R cells were grown in DMEM: F12 50:50 medium (Gibco: Thermo Fisher Scientific, Waltham, Massachusetts, USA) supplemented with 2.5 % NuSerum (Corning, #355100, Thermo Fisher Scientific, Waltham, Massachusetts, USA), penicillin/streptomycin (Gibco) and ITS Premix (Corning #354350). Of note, we used ITS instead of ITS+ , as the latter contains Bovine Serum Albumin (BSA) which was one of the additive substances evaluated in our experimental conditions [28]. Unless indicated, all experiments were conducted in the absence of serum. Cell lines were periodically tested for mycoplasmas and authenticated by genetic profiling through polymorphic short tandem repeat loci with the PowerPlex® 16 System (Promega, Madison, Wisconsin, USA) and Applied Biosystems 3130 genetic Analyzer (Thermo Fisher Scientific, Waltham, Massachusetts, USA).

2.3. RNA extraction

Total RNA was extracted from cell lines, either treated or not treated with mitotane. Genomic DNA contamination was removed by DNAse I treatment (Promega, Madison, Wisconsin, USA). RNA was then quantified via NanoDrop (Thermo Fisher Scientific, Waltham, Massachusetts, USA) and stored at −80°C.

2.4. RNA sequencing

Libraries were generated from total RNA using the Illumina TruSeq Stranded Total RNA Library Prep Gold and Novaseq 6000 System (Illumina), following the Illumina standards procedure and kits. FastP tool with default setting was utilized for quality control and preprocessing of FASTQ files that are essential to provide clean data for downstream analysis [30]. Subsequently, quantification of transcript expressions was generated by the Salmon algorithm (Ver 1.9.0, specific parameters: -l A -p 40 –validate Mappings –seqBias –gcBias), which considers experimental attributes and biases, commonly observed in real RNAseq data, to perform inferences on transcript expressions [31]. Next, the filtered counts' table was used as input to determine differential gene expression, performed using the program edgeR version 3.32.1 in R [32]. This procedure resulted in a gene list containing false discovery rate (FDR), p-value, and counts per million mapped reads (CPM). Genes with an absolute $|\log2FC= > 1$ (which corresponds to at least a 100 %-fold change) and FDR < 0.05 were considered differentially expressed genes (DEGs). These DEGs were used for subsequent analysis.

2.5. Functional enrichment analysis

Using the resulting list of DEGs obtained by key experimental contrasts, a functional analysis was performed using an enrichment tool included in the limma R Bioconductor package [33]. Goana and Kegga functions test for over-representation of Gene Ontology (GO) terms or KEGG pathways in one or more sets of genes, optionally adjusting for abundance or gene length bias [34]. The p-values returned by Goana and Kegga are unadjusted for multiple testing. The authors chose not to correct automatically for multiple testing because GO terms and KEGG pathways are often overlapping, so standard methods of p-value adjustment may be overly conservative. For this reason, the best results obtained in the enrichment analysis were tested with the Fry function that implements rotation gene set tests proposed by Wu et al. [35]. Pathways or GO terms were assumed to be enriched if the Fry test false discovery rate (FDR) was < 0.01. To visualize and investigate interesting enriched KEGG pathways, pathway gene annotation was performed using Pathview 3.19 [36]. In addition, to make inferences about the upstream regulator, responsible for transcriptional patterns specific to the most indicative biological contrasts, we utilized the QuaternaryProd R package. This algorithm computes the significance of upstream regulators in the network by performing causal reasoning using the Quaternary Dot Product Scoring Statistic (Quaternary Statistic) [37].

2.6. cDNA synthesis and droplet digital PCR (ddPCR)

2 μg of total RNA was reverse-transcribed with random hexamer primers and MultiScribe Reverse transcriptase (High Capacity cDNA Archive Kit, Applied Biosystems: Thermo Fisher Scientific), according to

the manufacturer's instructions. Different primers were designed to evaluate genes involved in the "Steroid hormone biosynthesis" pathway using Primer Express 2.0 (Thermo Fisher Scientific, Waltham, MA, USA). Primer efficiency was calculated for each transcript with RT–PCR (ABI Prism 7500 Sequence Detection System; Applied Biosystems) by using serial dilutions of cDNA of H295R. The specificity of each amplicon was evaluated by analyzing the respective melting curves (Supplementary file 1). In addition, to confirm the involvement of the ATF4 pathway we used "assays on demand" (Thermo Fisher Scientific, Waltham, Massachusetts, USA) for the following genes (Assay ID): ATF4 (Hs00909569_g1), CHAC1 (Hs00225520_m1), ASNS (Hs04186194_m1), PSAT1 (Hs00253548_m1) and ATF3 (Hs00231069_m1). Each sample was partitioned into ~20,000 droplets by a droplet generator (QX200™ Droplet Generator, Bio-Rad, Hercules, CA, USA), and each droplet was amplified by using ddPCR™ Supermix (for Probes or Evagreen) (Bio-Rad, Hercules, CA, USA), and the thermal cycling conditions suggested by the manufacturer. Custom primers were used at a final concentration of 100 nM, while the "assays on demand" were diluted following the manufacturer's indications. After the amplification, each sample was then loaded onto the QX200™ Droplet Reader (Bio-Rad, Hercules, CA, USA), and ddPCR data were analyzed with QX Manager™ analysis software (version 2.0, Bio-Rad, Hercules, CA, USA). Each sample was analyzed at least in biological duplicates for all the concentrations of mitotane in the study. The target concentration in each sample was expressed and normalized as a percentage of gene/*HRPT1* (Gene Ratio); the differential expression was evaluated relative to mitotane 0 μM (not treated cell line) and expressed as base 2 log of fold change ($\log_2$(Gene Ratio$_{[conc\ x]}$/Gene Ratio$_{[0\mu M]}$)). Statistical analysis was performed using t-tests with a significance level of $p < 0.05$, comparing each mitotane concentration versus the untreated control.

2.7. Western blot and protein analysis

To isolate total protein content, cells were lysed on ice with RIPA buffer (Thermo Fisher Scientific, Waltham, Massachusetts, USA) supplemented with Halt™ Protease and Phosphatase Inhibitors Single-Use Cocktail (Thermo Fisher Scientific, Waltham, Massachusetts, USA), and cell debris was removed by centrifugation at 16,000 × g at 4°C for 10 min. Evaluation of ATF4 expression was performed by Western Blot analysis. Equal amounts of protein (40 μg/well) for each sample were loaded and analyzed through SDS-PAGE (Any kD™ Mini-PROTEAN® TGX™ Precast Protein Gels, Bio-Rad). Proteins were then transferred onto PVDF membranes (Trans-Blot Turbo Mini 0.2 μm PVDF Transfer Packs, Bio-Rad) using Trans-Blot Turbo Transfer System and protocol recommended by the producer, blocked in EveryBlot Blocking Buffer (Bio-Rad) for 10 minutes and incubated overnight at 4°C with primary antibodies (1:1000 dilution in TBS-Tween20 0.3 %) against ATF4 (Cell Signaling Technology (CST), # 11815, Danvers, MA, USA) and Vinculin (CST, # 13901). Anti-rabbit IgG/HRP (CST, #7074) and anti-mouse IgG/HRP (CST, #7076) were used as secondary antibodies (1:8000 dilution). Enhanced chemiluminescence method (Clarity ECL, Bio-rad, Hercules, CA, USA) was used for protein-bound detection and the images were acquired using the ChemiDoc™ system (Bio-rad, Hercules, CA, USA).

3. Results

We have recently demonstrated that the presence of serum or BSA almost completely inhibits the biological activity of mitotane [28]. To elucidate, at the transcriptional level, the biological mechanisms influenced by mitotane treatment in an environment free from confounding factors, we treated the H295R cell line for 24 hours (h) with increasing concentrations of mitotane (0, 5, 10, 15, and 20 μM, respectively). For each mitotane concentration, we identified the genes differentially

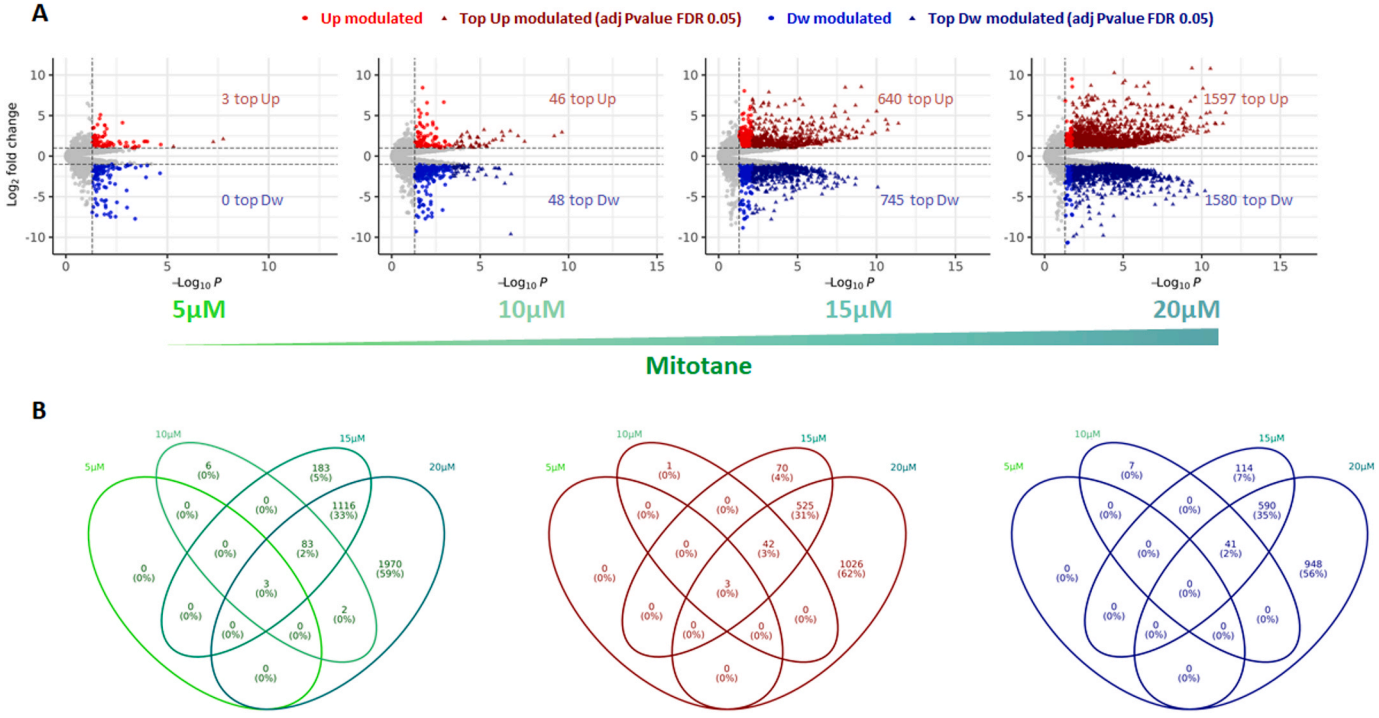

Fig. 1. Gene expression analysis of the differentially expressed genes. (A) Volcano plots showing the differentially expressed genes compared to untreated (NT) H295R (5μMvs.NT, 10μMvs.NT, 15μMvs.NT, 20 μMvs.NT). H295R cell line was treated with increasing mitotane concentration (0–5 – 10 – 15–20μM) for 24 h, in absence of serum. Up-modulated genes were indicated as red dots, down-modulated genes as blue dots; the genes that satisfied the conditions of $\log_{10}P = \pm 1$ and FDR 0.05 were indicated in dark red and dark blue, with also the respective number on each graph. (B) Overlaps of the identified DEGs between the different mitotane concentrations in general (green graph) and dividing them between upregulated and downregulated genes (red and blue graphs, respectively).

expressed compared to untreated H295R (NT). The volcano plots in Fig. 1A show the results of this analysis. As expected, the number of differentially expressed genes (DEGs) rose with increasing mitotane concentration, from a few to a few dozen for the first two concentrations and to thousands at the highest ones (Fig. 1A, dark red dots). Focusing on gene regulation, we observed that the number of upmodulated genes (red dots) was approximately the same as that of the downmodulated ones (Fig. 1A, dark blue dots) for each of the experimental contrasts considered. In Fig. 1B, we can observe the overlaps of the identified DEGs between the different mitotane concentrations, both as a general overview (Fig. 1B, green graph) and by dividing them between upregulated and downregulated genes (Fig. 1B, red and blue graphs, respectively). Again, the proportion of upmodulated and downmodulated genes appeared to be the same for each intersection.

There was a direct trend between the number of differentially expressed genes and the mitotane concentration used over 24 h (Pearson's correlation = 0.94; p-value = 0.058). This could indicate that certain genes are progressively regulated by increasing mitotane concentrations. To evaluate this, we performed a multivariate analysis across all mitotane concentrations to identify genes that were either upregulated or downregulated. We assessed two different scenarios: in the first, the untreated cells were used as a baseline ("normalizer") and the gene expression trend was evaluated across the experimental contrasts (5 μM/NT -> 10 μM/NT -> 15 μM/NT -> 20 μM/NT). The top 300 genes identified with this approach are depicted in Fig. 2A and B, showing a notable divergence in gene expression starting at 10 μM mitotane compared to untreated cells, with maximal regulation observed at the highest concentrations (Fig. 2A and B, Supplementary file 2).

In the second approach, shown in Fig. 2C and D, we used the previous mitotane concentration as the "normalizer" of each experimental contrast (5 μM/NT -> 10 μM/5 μM -> 15 μM/10 μM -> 20 μM/15 μM). This analysis was useful for identifying when gene expression changes peaked or plateaued. Interestingly, many genes showed maximum expression levels at 15 μM mitotane after 24 h, which then either stabilized or decreased at 20 μM (Fig. 2C and D). A detailed list of DEGs and their transcriptional regulations for each comparison is provided in the supplementary data (Supplementary file 2).

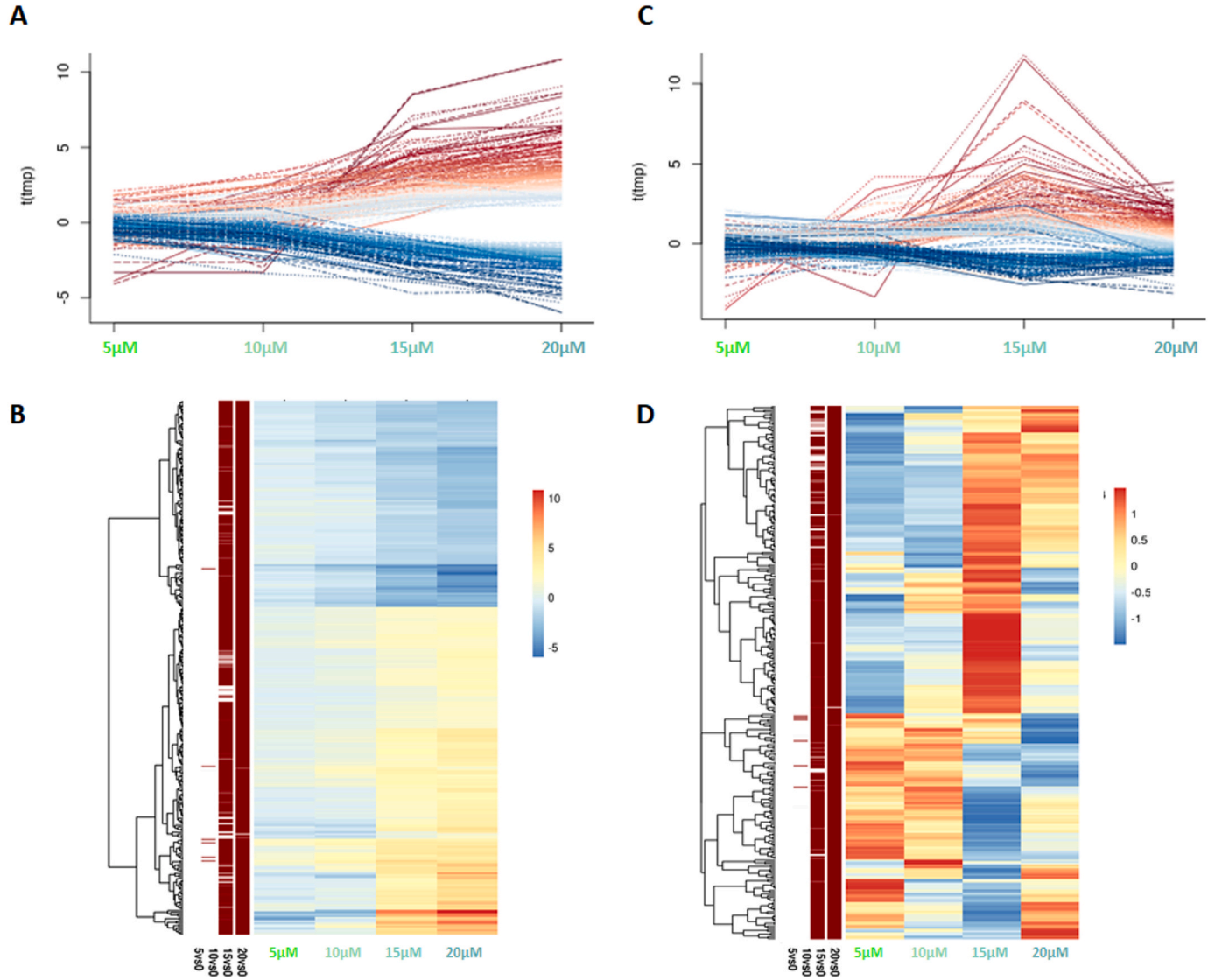

Fig. 2. Multivariate analysis of the top 300 differentially expressed genes. The graph (A) and the heatmap (B) show the results of multivariate analysis using the untreated condition as the "normalizer" to evaluate the tendency of gene expression across the experimental contrasts (5 μM/NT -> 10 μM/NT -> 15 μM/NT -> 20 μM/NT). The graph (C) and the heatmap (D) show the results of multivariate analysis using the previous concentration of mitotane as the "normalizer" of each experimental contrast (5 μM/NT -> 10 μM/5 μM -> 15 μM/10 μM -> 20 μM/15 μM). The p-values of the indicated contrast are shown on a red scale.

3.1. GO and KEGG enrichment analysis

Fig. 3 provides an overview of the Gene Ontology (GO) analysis performed on the DEGs identified in the previous analyses, as tabulated in Supplementary file 3. A word cloud highlights the most frequent GO terms, including "cellular component", "cellular anatomical entity" and "extracellular region" (Fig. 3A), which were enriched across most experimental contrasts. Fig. 3B shows the top 20 enriched terms identified in the multivariate analysis, illustrating the course of gene regulation (Fig. 3B, bubble plot). In the lower panels, we highlighted the top 20 GO enrichments for experimental contrasts indicative of mitotane-mediated gene expression: the point at which its transcriptional effect first became evident, 10 μM for 24 h (Fig. 3C, bubble plot), and the concentration with the highest number of deregulated genes (mitotane 20 μM for 24 h) (Fig. 3D, bubble plot).

Since the same gene can be associated with multiple GO terms, the p-values of the initial analysis were not adjusted for multiple testing. To overcome this, we performed a more stringent enrichment analysis using the FRY test, which considers unique genes. This test, combined with FDR correction, also indicated the predominant direction of the pathway regulation (UP or DOWN modulated). The trend of gene expression across the concentration gradient was enriched with terms such as "response to stimuli", "chemical agents" and "regulation of biological processes", such as "cell migration" or "developmental processes". Noteworthy was the difference in GO term enrichment between 10 and 20 μM. In the first case (10 μM), metabolic processes, including "sterol biosynthesis", "cholesterol", "lipids" and/or "steroids", seemed to be turned off (for all analyses, FRY test FDR<<0.01 trend DOWN). In the second case (20 μM), metabolic processes shift towards reduced activity in favor of pathways like "nucleotide biosynthesis", including "phosphate nucleotides", while GO terms became more focused on "cell membranes" and "mitochondrial". In particular, the mitochondrion appeared to be a key target, with downregulated activities related to the "mitochondrial membrane", including "ATP synthesis coupled to electron transport", "aerobic respiration" and "oxidative phosphorylation" (all indicated terms were predominantly downmodulated with FRY test FDR <<0.01).

The same analysis was performed to observe the enrichment of the metabolic pathways included in the KEGG database (Fig. 4 and tabulated in Supplementary file 4). The most prominent pathways in the analysis were “Biosynthesis of amino acids”, “Metabolic pathways”, and “Glutathione metabolism”, which we observed both in the multivariate analysis and in the different experimental contrasts (Fig. 4A and B). The metabolic pathways enriched in the KEGG database confirmed what was observed in the previous paragraph of the Gene Ontology. The gene trends focused on “lipids”, “atherosclerosis”, and various syntheses, including that of “steroids”, the “metabolism of mannose”, “glutathione” and “xenobiotics”. Interestingly, mitotane downmodulated the pathways involved in chemical carcinogenesis, in particular, the “production of adducts”, in “ferroptosis” and “cellular senescence”, were observed as significant also at mitotane concentrations of 15 and 20 μM. Even in the case of specific contrasts at 10 and 20 μM (Fig. 4C and D, respectively), we observed a behavior similar to the GO analysis. In particular, at the lowest concentration, we observed a significant downmodulation of pathways involving the synthesis of “terpenoids”, which are precursors of sterols, and the metabolism and excretion of “fats and fatty acids”, synthesis of “cortisol”, “aldosterone”, and “steroid hormones” (all indicated pathways were predominantly downmodulated with FRY test FDR <<0.01). At the highest concentration, we still observed the downmodulation of “steroid synthesis”, but the majority of pathways seemed to converge on the inhibition of “oxidative phosphorylation” and “chemical carcinogenesis”, such as the production of “reactive oxygen species/DNA adducts” and processes related to “oxidative phosphorylation” such as “thermogenesis” (all predominantly downmodulated with FRY test FDR <<0.01). GO/KEGG full tables and some representative specific pathways were included in Supplementary file 3, 4, and 5.

Transcriptional analysis provides us with information about the genes activated by one or more regulators and transcription factors, without telling us which ones are responsible for the observed pattern. To predict the putative upstream regulators affected by mitotane, we used the R package QuaternaryProd. This algorithm, for a given set of differentially expressed genes, calculates the significance of the upstream regulators in the network using the quaternary dot product score statistic. We analyzed all genes upregulated by the contrast at 10 μM with this QuaternaryProd and observed that the most significant upstream regulators were the genes *ATF4* and *MAPK8* (both p-value <<0.01). To confirm this result, we examined genes indicated in the literature as targets of Activating transcription factor 4 (ATF4) [38–43], including *CHAC1, ASNS, PSAT1*, and *ATF3*. All these genes were upmodulated in our analysis, consistent with ATF4 activity. Among these, CHAC1, ASNS, and PSAT1 were early mitotane responders, exhibiting upmodulation at all the concentrations used in our analysis (*CHAC1* log2(FC) 2–4, FDR < <0.01; *ASNS* log2(FC) 1.7–3.1, FDR < <0.01; *PSAT1* log2(FC) 1.2–2.2, FDR < 0.02). In contrast, *ATF3* was not significantly regulated at the lowest concentration, but it was the most upmodulated gene observed in both the highest mitotane concentrations, with the highest upregulation trend (15 μM log2(FC) 4.48 FDR < <0.01, 20 μM log2(FC) 5.35 FDR < <0.01 and trend FDR < <0.01).

Mitotane likely deregulates a plethora of transcription factors. In an attempt to reduce the complexity of the DEGs model and to identify specific regulators, we ran QuaternaryProd with a subset of the DEGs. In particular, we selected genes present in the specific KEGG pathways enriched in our analysis at mitotane 20 μM, a concentration with the highest number of deregulated genes in KEGG pathways. To limit biases due to transcriptional pattern sub-selections, we reported here the genes that were present only in multiple KEGG metabolic pathways. Notably, we observed that POMC (Pro-opiomelanocortin) could be a good upstream regulator candidate for the KEGG pathways “Steroid hormone biosynthesis”, “Aldosterone synthesis and secretion”, and “Cortisol synthesis and secretion”. In contrast, members of the SREBF family were significantly suppressed for KEGG pathways, specifically “Biosynthesis of unsaturated fatty acids” and “Fatty acid metabolism” for SREBF1, and “Steroid biosynthesis” and “Terpenoid backbone biosynthesis” for SREBF2.

To confirm this data, we repeated the experiments in H295R, performing at least in biological duplicates, and we re-evaluated the transcriptional pattern of “Steroid hormone biosynthesis” and ATF4 pathway using ddPCR technology. Fig. 5 shows the results for six key genes involved in the “steroid hormone biosynthesis” pathway, where RNAseq analysis showed a clear down-modulation. Except *CCN3*, which exhibited significant downmodulation only at 10 μM, the remaining genes appeared to correlate almost perfectly with the RNAseq analysis results. Almost all transcripts were halved already at 5 μM, and many of these reached their maximum shutdown at 15 or 20 μM. In particular, for *CYP21A2*, *CYP17A1,* and *STAR* we could appreciate the coupled trend between the two analyses, which trace the same pattern of gene expression (Fig. 5).

Similar results were observed for ATF4 pathway (Fig. 6A). Indeed, the regulations observed in ddPCR were consistent with RNAseq analysis for the AFT4 pathway genes deregulated in response to mitotane. In particular, the early activation of *ASNS*, *CHAC1*, and *PSAT1* genes was evident from the significant rapid up-modulation already at 5 μM, with intensities even higher than those observed in the omics analysis (for all $p < 0.01$). Furthermore, we evaluated the transcriptional activation of ATF4 (Fig. 6B). Although mitotane treatment resulted in ATF4 overexpression, the statistical significance and intensity of this regulation at the transcript levels were near the threshold limits of our analysis. This finding aligns with the RNAseq results. In contrast, at the protein level, we observed a clear modulation of the ATF4 in response to mitotane treatment. Indeed, the levels of this protein, undetectable in the untreated H295R cell line, became evident with increasing concentration of the drug (Fig. 6B). This upmodulation of the ATF4 protein further

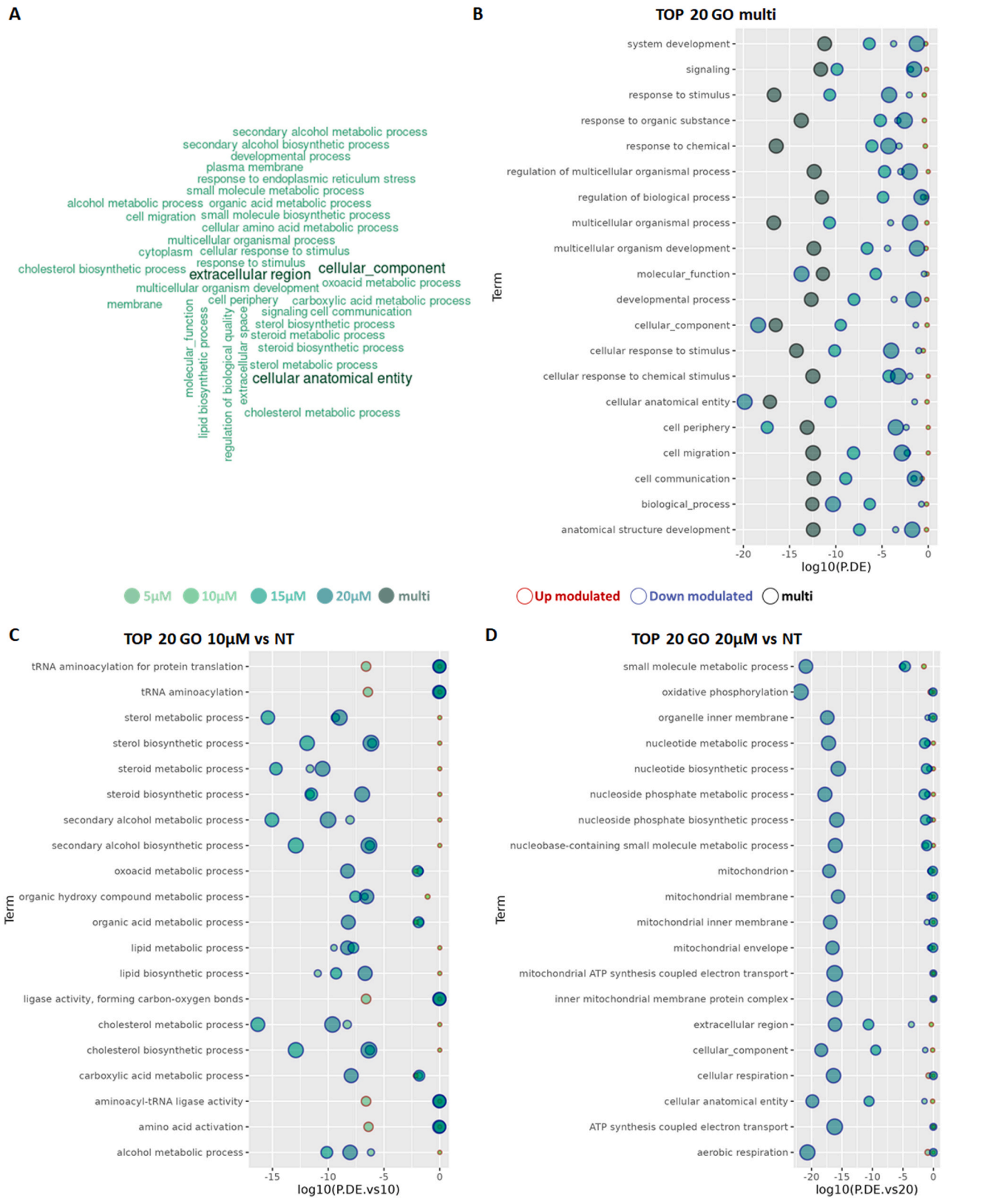

Fig. 3. Gene Ontology (GO) enrichment analysis of the differentially expressed genes. (A) The word cloud highlights the frequencies of the GO pathways across the contrasts of all concentrations. The most frequent pathways are displayed in darker colors and indicated with a larger font size. The Bubble plots list the 20 most significant GO pathways obtained from the multivariate analysis (B), from the minimum contrast in which we see the divergence of gene regulation, 10 μM (C), and from the maximum contrast 20 μM (D). Bubble plots indicate the percentage of regulated genes in each pathway (circle size), whether the differential genes expressed in the pathway are more upregulated (red border) or downmodulated (blue border), and the significance of these p-values in the various contrasts (most significant = closest to the name of the pathway).

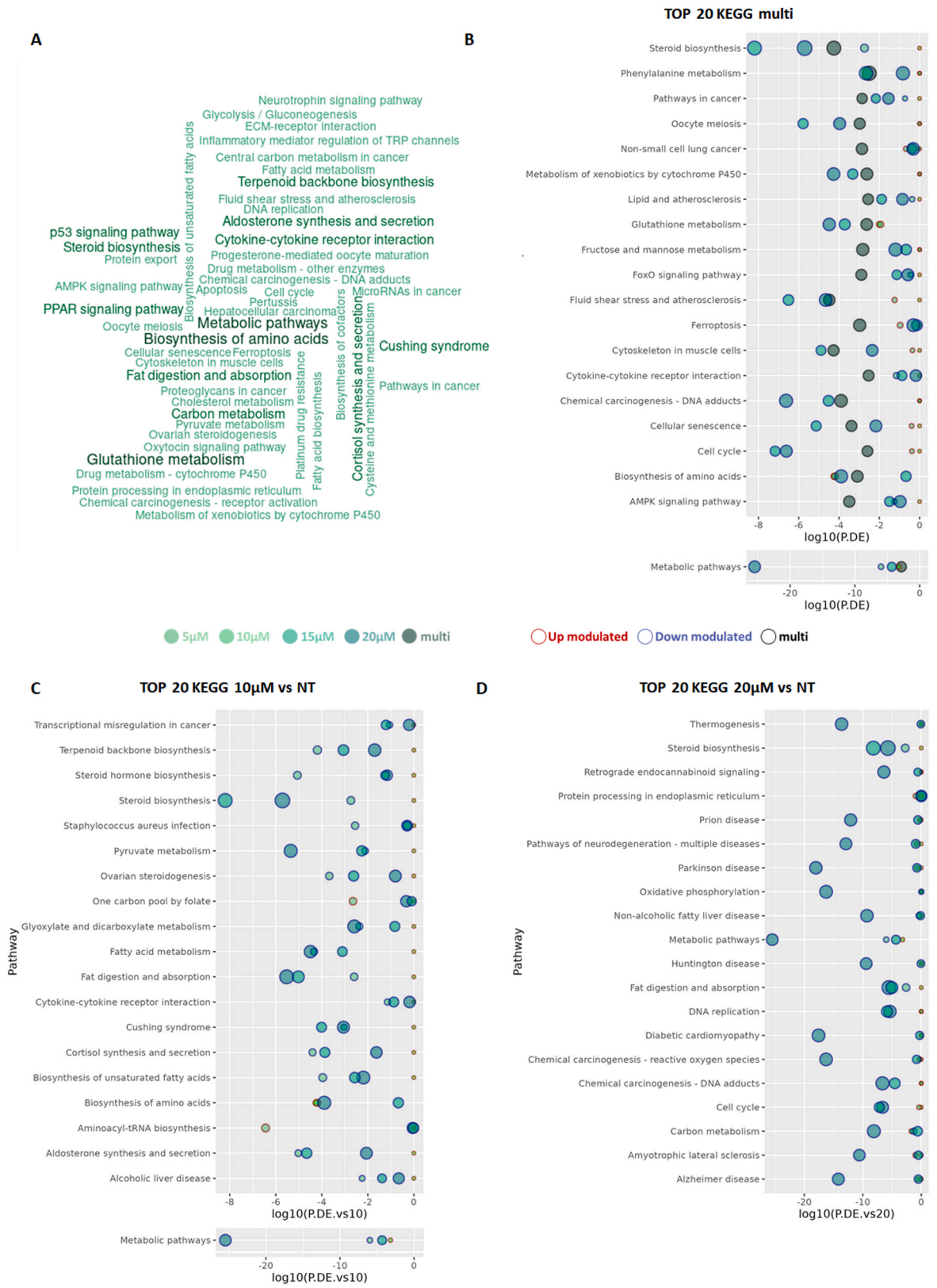

Fig. 4. KEGG enrichment analysis of the differentially expressed genes. The word cloud (A) highlights the frequencies of the KEGG pathways present in the contrasts of all concentrations. The most present pathways are darker and indicated with a larger font. The following images list the 20 most significant KEGG pathways obtained from the multivariate analysis (B), from the minimum contrast in which we see the divergence of gene regulation, 10 µM (C), and from the maximum contrast 20 µM (D). Bubble graphs indicate the percentage of genes regulated in each pathway (circle size), whether the differential genes expressed in the pathway are more upregulated (red border) or downmodulated (blue border) and the significance of these p-values in the various contrasts (most significant = closest to the name of the pathway).

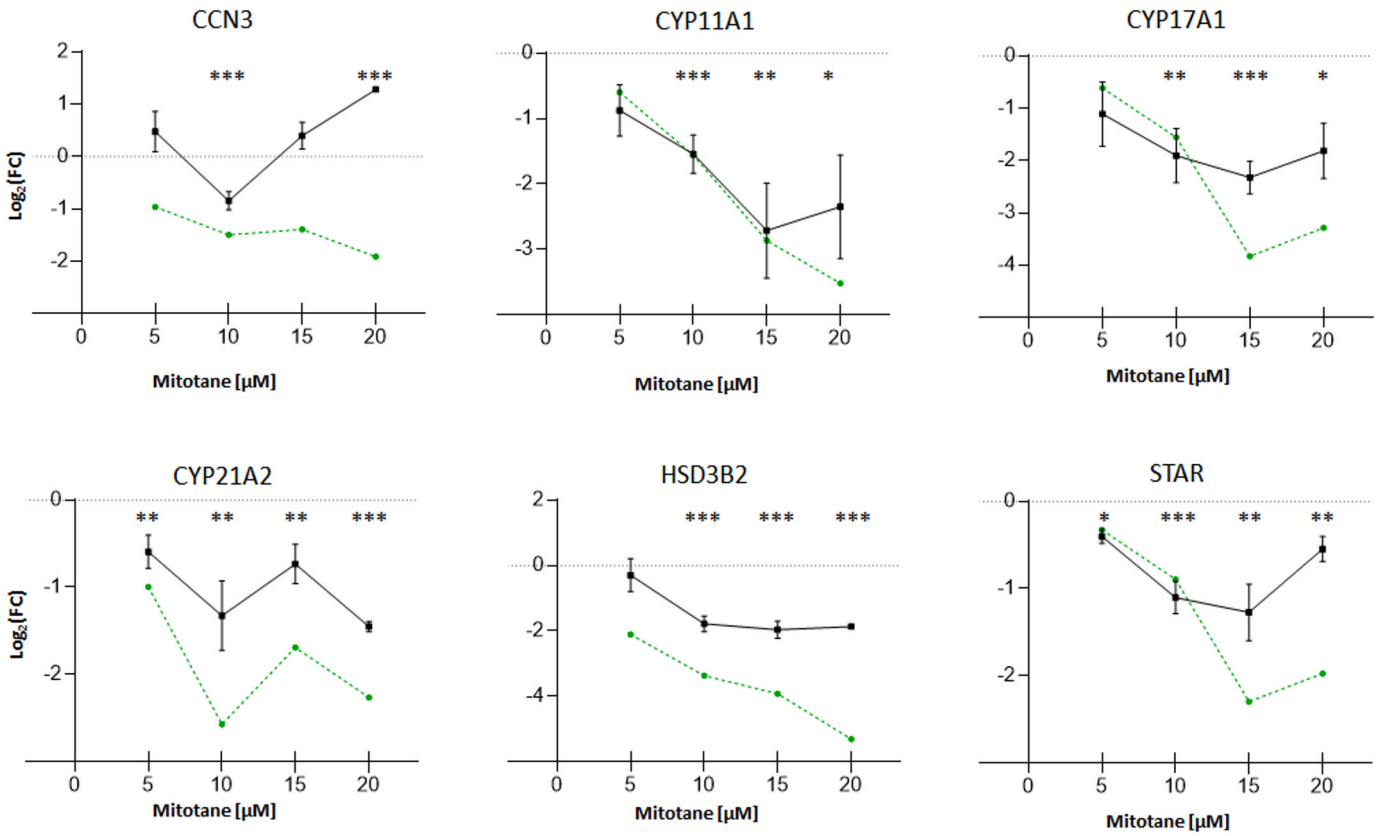

Fig. 5. Effect of mitotane on the gene expression of the "steroid hormone biosynthesis" pathway. CCN3, CYP11A1, CYP17A1, CYP21A2, HSD3B2 and STAR gene expression patterns obtained with ddPCR quantification (black line) coupled to their respective RNAseq analysis (green dashed line). Except for CCN3, we observed an almost perfect correlation with the RNAseq data, with a clear overall downmodulation. ddPCR and RNAseq results were expressed as $\log_2$ of the fold change ($\log_2$[FC]= $\log_2$[Gene Ratio$_{[\text{conc x}]}$/Gene Ratio$_{[0\mu M]}$]). * Indicates a trend p-value ≤ 0.1; ** indicates a p-value < 0.05; *** indicates a p-value < 0.01.

supports the involvement of this pathway in the biological activity of mitotane.

4. Discussion

A controlled environment, free from confounding factors, is essential to study the pharmacological effect of any drug. Under such conditions, it becomes possible to identify the primary targets early and expand the knowledge of the active compounds (or molecules) acting on them. On these bases, we evaluated the transcriptional pattern of mitotane in the H295R cell line, in the absence of BSA and serum, as both interact with mitotane and block its biological activity [28]. This approach allowed us to observe a remarkable genetic deregulation with exposure to mitotane concentrations ten times lower than those reported in the current literature, within a 24 h exposure interval. Consequently, we observed initial deregulations even at lower mitotane concentrations, with a clear distinction from untreated cells, particularly at 10 µM after 24 h.

Interestingly, we did not observe significant differences in the direction (up or down) of gene deregulation across the various experimental contrasts analyzed, whether evaluating the contrasts individually or examining the transcriptional trends. Indeed, across the different mitotane concentrations, we observed a rather good symmetry between the genes that were up and downmodulated after 24 h. However, when analyzing the enrichment of KEGG pathways or GO terms, we noticed that most of the enriched pathways were characterized by a predominant gene downmodulation, with only a few upmodulated genes, often detected at the highest concentrations tested. Our analysis indicated that mitotane was responsible for the systematic suppression of several pathways crucial for the adrenal cortex cells. A key target appeared to be the mitochondrial processes, starting with specific pathways, such as those responsible for steroid hormone synthesis and related genes. This suppression extended to the deregulation of pathways essential for oxidative respiration, ultimately impairing the primary functions of the mitochondrion itself.

Our analysis confirmed, at both RNAseq and ddPCR levels, the known mitotane-mediated downmodulation of different genes such as *STAR*, *CYP11A1*, *CYP21A2*, and *HSD3B2* [26,27,44–46], even after just 24 h. Intriguingly, although a significant regulatory trend was evident, marked downregulation was only observed at the highest concentrations tested. The deregulation of CYP11B1 isoforms appears to be more complex, with literature data reporting controversial findings. Depending on the experimental conditions, CYP11B1 has been observed as either downmodulated [27,47,48] or upmodulated following mitotane treatment [46]. In contrast, the *CYP11B2* gene is consistently reported to be transcriptionally inhibited by mitotane *in vitro* [27]. In our analysis, CYP11B1 was not deregulated under any of our experimental conditions, and no trend was observed. Similarly, CYP11B2 was not significantly deregulated at any tested concentrations, though we observed a trend in gene regulation. This trend ranged from upregulation at the two lowest concentrations to downregulation at the two highest concentrations. The behavior of all these genes implicated in steroid hormone biosynthesis suggests that their deregulation might not occur immediately, but may require a priming process to reinforce their downmodulation over time. In this scenario, understanding the primary drivers of this transcriptional regulation could be crucial for identifying druggable metabolic pathways and developing new drugs.

We identified POMC as a specific upstream modulator. Previous studies have found that mitotane reduces POMC expression and blocks the stimulatory effects of corticotropin-releasing hormone on pituitary cell viability [49]. In our analysis, we did not observe deregulations of

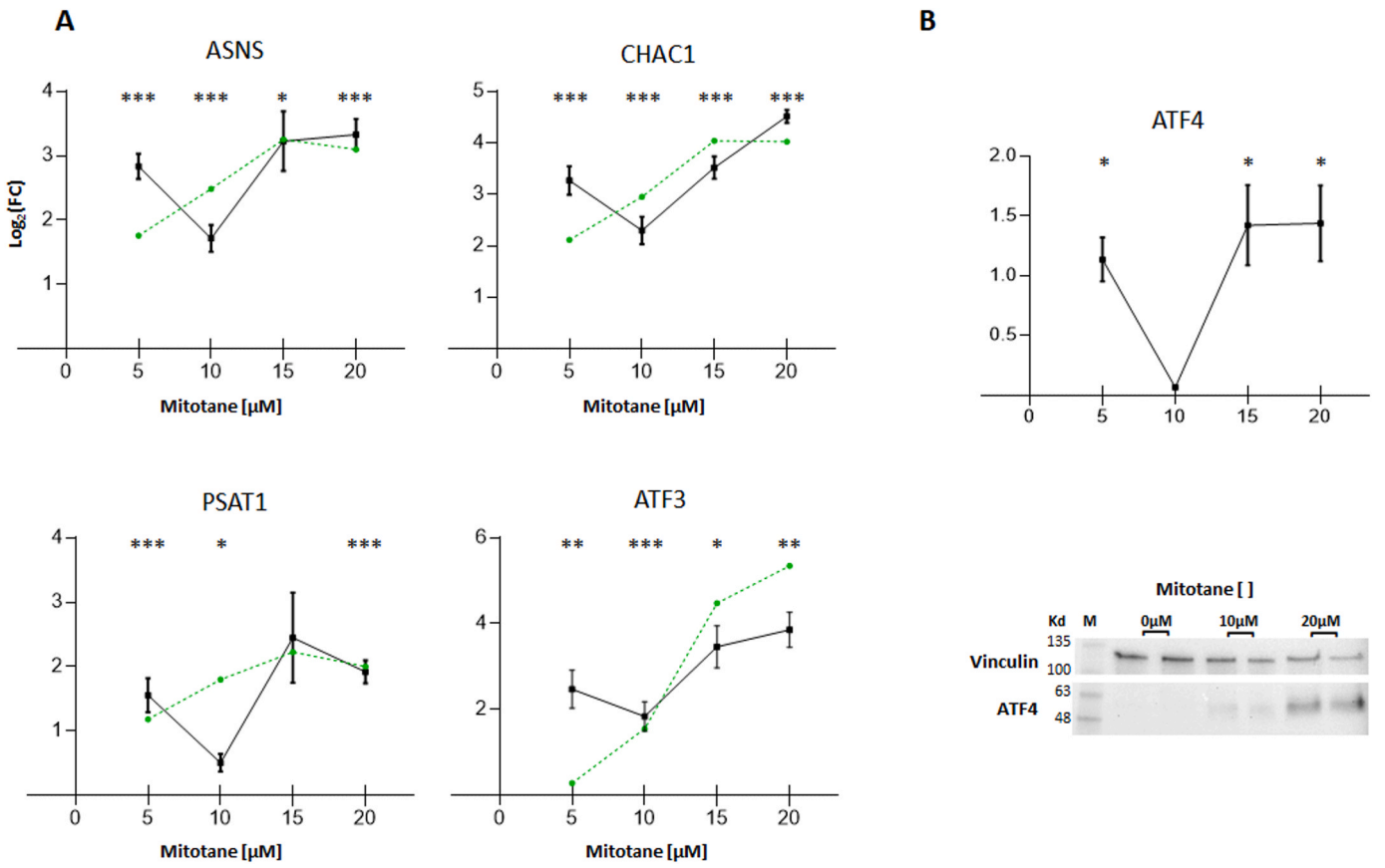

Fig. 6. Effect of mitotane on the ATF4 pathway. (A) *ASNS*, *CHAC1*, *PSAT1*, and *ATF3* gene expression was evaluated to validate RNAseq data, suggesting the possible involvement of the ATF4 pathway. For all the genes, the expression patterns obtained with ddPCR quantification (black line) showed a perfect correlation with the coupled RNAseq analysis (green dashed line). ddPCR and RNAseq results were expressed as log2 of the fold change (log2[FC]= log2[Gene Ratio[conc x]/Gene Ratio [0 μM]]). * Indicates a trend p-value ≤ 0,1; * * indicates a p-value < 0,05; * ** indicates a p-value < 0,01. (B) ddPCR quantification of ATF4 gene expression regulation induced by mitotane treatment (curve concentration 0–5 – 10 – 15–20 μM). * Indicates a trend p-value ≤ 0,1. ATF4 upregulation was confirmed by Western blot analysis. H295R cells were cultured in the absence of serum for 24 h with mitotane 0–10–20 μM. A 40 μg volume of protein lysate from each condition in biological replicate was evaluated decorating with ATF4 antibody (49 kDa) or Vinculin (120 Kd). We observed a clear up-modulation of ATF4 protein increasing drug concentration.

this gene, although mitotane appeared to act as a repressor of this pathway in ACC cells. Furthermore, we observed that other possible upstream regulators could be the SREB family genes. In our experiment, both *SREB1* and *SREB2* genes were specifically downmodulated, along with the pathways dependent on them. Our findings are in line with those previously reported by Sbiera et al., who identified "SCAP/SREBF transcriptional control of cholesterol and fatty acids biosynthesis" as one of the main mitotane-deregulated pathways regulated by the SREB family [25]. Interestingly, the same study also highlighted SOAT1 as a key molecular target of mitotane, whose inhibition induces ER stress and could serve as a predictive marker of drug response [25,50]. In contrast, our analysis found that SOAT1 was not an early responsive gene to mitotane treatment. Significant downmodulation was observed only at the highest concentration, with a mere trend at lower doses. We hypothesize that this lack of strict dependence on mitotane treatment could explain the failure of SOAT assessment to predict mitotane response in patients with ACC in subsequent studies [51,52].

Our analysis also supports the hypothesis that mitotane induces ER stress, although our data suggest new key targets. Increased ER stress and unfolded protein response (UPR) indicated changes in the cellular environment, often due to disturbances in cellular metabolism. In our analysis, we observed the activation of several key transcription factors involved in the UPR, including *ATF4*, *ATF6*, and *XBP1* [40], with varying degrees of significance. In our work, mitotane appeared to mediate this process by triggering a cell death cascade event that involved the ER, mitochondrial membrane, and oxidative stress. As early as 5 μM for 24 h, we observed the upmodulation of *CHAC1*, *ASNS*, and *PSAT1* in both analyses, and these genes were also significantly upmodulated at all higher concentrations tested. In addition, *ATF3* was the most upmodulated gene, particularly at the highest mitotane concentrations, showing the strongest upregulation trend. This genetic behavior, as suggested by our inferential and protein analysis, appeared to affect the signaling axis involving the transcriptional factor ATF4. This gene, functioning both as a transcriptional activator and inhibitor, can be upregulated in response to various types of cell stress, including ER stress, oxidative stress, amino acid depletion, and integrated stress response [53]. Its role in regulating these genes is well-established [38–43]. In models found in the literature, ATF4 induces expression of ATF3, followed, at least in the case of amino acid deprivation, by ATF3 enhancing CHOP expression [38]. Literature data also suggest that CHAC1 is an important downstream target of the ATF4-ATF3-CHOP pathway, promoting apoptosis in response to oxidized phospholipids [40]. While the role of ATF4 in inducing ferroptosis is currently debated, it seems to promote it through the activation of NUPR1 and inhibit it via the pathway involving CHAC1 (reviewed in Tang et al.l. [53]). In our study, mitotane upmodulated both these genes, even though the drug has not been previously found to cause ferroptosis [54,55]. Furthermore, we observed a clear modulation of ATF4 protein levels in response to mitotane treatment. This finding confirms the transcriptional cascade observed in our RNAseq analysis and highlights how this pathway could

be important for the biological effect of mitotane. Further studies will be needed to define how modulation of ATF4 and its effectors might influence mitotane-mediated insult in ACC cells. The necessity to further investigate this molecular pathway is also underlined by a very recent study that identified the ATF family, particularly the high protein expression of ATF4, as an unfavorable prognostic marker in ACC (pre-print under review https://doi.org/10.21203/rs.3.rs-4278365/v1).

In conclusion, to the best of our knowledge, this is the first study to evaluate the transcriptional deregulation induced by mitotane in H295R cells in the absence of confounding factors that could alter its biological activity. Through our approach, we identified the main pathways that are deregulated by mitotane as early as 24 h post-treatment. While some of these pathways have been previously linked to mitotane treatment with mixed success, even at extreme mitotane concentrations, we identify the ATF4 pathway as one of the first molecular pathways triggered by mitotane, both at the protein and transcriptional levels. Some of these effectors could potentially be exploited in the future to identify functional biomarkers for treatment monitoring or as new pharmacological targets for ACC.

Funding

This work was supported by Associazione Italiana per la Ricerca sul Cancro (AIRC), grant number IG2019–23069 to Massimo Terzolo.

CRediT authorship contribution statement

Pignochino Ymera: Methodology, Formal analysis. **Giordano Giorgia:** Methodology, Data curation. **Ferrero Giulio:** Formal analysis. **Puglisi Soraya:** Data curation. **Tucciarello Cristina:** Methodology, Data curation. **Terzolo Massimo:** Writing – original draft, Supervision, Funding acquisition, Conceptualization. **Reimondo Giuseppe:** Data curation. **Saba Laura:** Writing – original draft, Methodology, Investigation. **Schiavon Aurora:** Writing – original draft, Methodology, Investigation, Conceptualization. **Lo Iacono Marco:** Writing – original draft, Supervision, Formal analysis, Data curation, Conceptualization. **Petiti Jessica:** Writing – original draft, Methodology, Investigation, Conceptualization. **Evaristo Carlotta:** Methodology.

Declaration of Competing Interest

The authors declare that they have no known competing financial interests or personal relationships that could have appeared to influence the work reported in this paper.

Appendix A. Supporting information

Supplementary data associated with this article can be found in the online version at doi:10.1016/j.biopha.2025.117917.

Data availability

Data will be made available on request.

References

[1] M. Fassnacht, G. Assie, E. Baudin, G. Eisenhofer, C. de la Fouchardiere, H.R. Haak, R. de Krijger, F. Porpiglia, M. Terzolo, A. Berruti, E.G.C.E.a. clinicalguidelines@esmo.org, Adrenocortical carcinomas and malignant phaeochromocytomas: ESMO-EURACAN Clinical Practice Guidelines for diagnosis, treatment and follow-up, Ann. Oncol. 31 (11) (2020) 1476–1490, https://doi.org/10.1016/j.annonc.2020.08.2099.

[2] M. Daher, J. Varghese, S.K. Gruschkus, C. Jimenez, S.G. Waguespack, S. Bedrose, L. Altameemi, H. Bazerbashi, A. Naing, V. Subaiah, M.T. Campbell, A.Y. Shah, M. Zhang, R.A. Sheth, J.A. Karam, C.G. Wood, N.D. Perrier, P.H. Graham, J.E. Lee, M.A. Habra, Temporal trends in outcomes in patients with adrenocortical carcinoma: a multidisciplinary referral-center experience, J. Clin. Endocrinol. Metab. 107 (5) (2022) 1239–1246, https://doi.org/10.1210/clinem/dgac046.

[3] M. Fassnacht, S. Johanssen, M. Quinkler, P. Bucsky, H.S. Willenberg, F. Beuschlein, M. Terzolo, H.H. Mueller, S. Hahner, B. Allolio, G. German Adrenocortical Carcinoma Registry, T. European Network for the Study of Adrenal, Limited prognostic value of the 2004 International Union Against Cancer staging classification for adrenocortical carcinoma: proposal for a Revised TNM Classification, Cancer 115 (2) (2009) 243–250, https://doi.org/10.1002/cncr.24030.

[4] S. Puglisi, A. Calabrese, F. Ferrau, M.A. Violi, M. Lagana, S. Grisanti, F. Ceccato, C. Scaroni, G. Di Dalmazi, A. Stigliano, B. Altieri, L. Canu, P. Loli, R. Pivonello, E. Arvat, V. Morelli, P. Perotti, V. Basile, P. Berchialla, S. Urru, C. Fiori, F. Porpiglia, A. Berruti, A. Pia, G. Reimondo, S. Cannavo, M. Terzolo, New findings on presentation and outcome of patients with adrenocortical cancer: results from a National Cohort Study, J. Clin. Endocrinol. Metab. 108 (10) (2023) 2517–2525, https://doi.org/10.1210/clinem/dgad199.

[5] R. Libe, O. Huillard, Adrenocortical carcinoma: diagnosis, prognostic classification and treatment of localized and advanced disease, Cancer Treat. Res Commun. 37 (2023) 100759.

[6] S. Puglisi, P. Perotti, A. Pia, G. Reimondo, M. Terzolo, Adrenocortical carcinoma with hypercortisolism, Endocrinol. Metab. Clin. North Am. 47 (2) (2018) 395–407.

[7] A. Sada, T.R. Foster, R. Al-Ward, S. Sawani, H. Charchar, R. Pishdad, A. Ben-Shlomo, B.M. Dy, M.L. Lyden, E. Bergsland, S. Jasim, N. Raj, J.B. Shank, O. Hamidi, A.H. Hamrahian, J.L. Chambo, V. Srougi, M.C. Fragoso, P.H. Graham, M.A. Habra, I. Bancos, T.J. McKenzie, The effect of hormonal secretion on survival in adrenocortical carcinoma: a multi-center study, Surgery 175 (1) (2024) 80–89, https://doi.org/10.1016/j.surg.2023.04.070.

[8] G.A. Margonis, Y. Kim, T.B. Tran, L.M. Postlewait, S.K. Maithel, T.S. Wang, J. A. Glenn, I. Hatzaras, R. Shenoy, J.E. Phay, K. Keplinger, R.C. Fields, L.X. Jin, S. M. Weber, A. Salem, J.K. Sicklick, S. Gad, A.C. Yopp, J.C. Mansour, Q.Y. Duh, N. Seiser, C.C. Solorzano, C.M. Kiernan, K.I. Votanopoulos, E.A. Levine, G. A. Poultsides, T.M. Pawlik, Outcomes after resection of cortisol-secreting adrenocortical carcinoma, Am. J. Surg. 211 (6) (2016) 1106–1113, https://doi.org/10.1016/j.amjsurg.2015.09.020.

[9] G. Abiven, J. Coste, L. Groussin, P. Anract, F. Tissier, P. Legmann, B. Dousset, X. Bertagna, J. Bertherat, Clinical and biological features in the prognosis of adrenocortical cancer: poor outcome of cortisol-secreting tumors in a series of 202 consecutive patients, J. Clin. Endocrinol. Metab. 91 (7) (2006) 2650–2655, https://doi.org/10.1210/jc.2005-2730.

[10] J. Crona, F. Beuschlein, Adrenocortical carcinoma - towards genomics guided clinical care, Nat. Rev. Endocrinol. 15 (9) (2019) 548–560.

[11] G. Assie, E. Letouze, M. Fassnacht, A. Jouinot, W. Luscap, O. Barreau, H. Omeiri, S. Rodriguez, K. Perlemoine, F. Rene-Corail, N. Elarouci, S. Sbiera, M. Kroiss, B. Allolio, J. Waldmann, M. Quinkler, M. Mannelli, F. Mantero, T. Papathomas, R. De Krijger, A. Tabarin, V. Kerlan, E. Baudin, F. Tissier, B. Dousset, L. Groussin, L. Amar, E. Clauser, X. Bertagna, B. Ragazzon, F. Beuschlein, R. Libe, A. de Reynies, J. Bertherat, Integrated genomic characterization of adrenocortical carcinoma, Nat. Genet 46 (6) (2014) 607–612.

[12] S. Zheng, A.D. Cherniack, N. Dewal, R.A. Moffitt, L. Danilova, B.A. Murray, A. M. Lerario, T. Else, T.A. Knijnenburg, G. Ciriello, S. Kim, G. Assie, O. Morozova, R. Akbani, J. Shih, K.A. Hoadley, T.K. Choueiri, J. Waldmann, O. Mete, A. G. Robertson, H.T. Wu, B.J. Raphael, L. Shao, M. Meyerson, M.J. Demeure, F. Beuschlein, A.J. Gill, S.B. Sidhu, M.Q. Almeida, M. Fragoso, L.M. Cope, E. Kebebew, M.A. Habra, T.G. Whitsett, K.J. Bussey, W.E. Rainey, S.L. Asa, J. Bertherat, M. Fassnacht, D.A. Wheeler, N. Cancer Genome Atlas Research, G. D. Hammer, T.J. Giordano, R.G.W. Verhaak, Comprehensive pan-genomic characterization of adrenocortical carcinoma, Cancer Cell 30 (2) (2016) 363, https://doi.org/10.1016/j.ccell.2016.07.013.

[13] J.A. Glenn, T. Else, D.T. Hughes, M.S. Cohen, S. Jolly, T.J. Giordano, F.P. Worden, P.G. Gauger, G.D. Hammer, B.S. Miller, Longitudinal patterns of recurrence in patients with adrenocortical carcinoma, Surgery 165 (1) (2019) 186–195, https://doi.org/10.1016/j.surg.2018.04.068.

[14] I. Erdogan, T. Deutschbein, C. Jurowich, M. Kroiss, C. Ronchi, M. Quinkler, J. Waldmann, H.S. Willenberg, F. Beuschlein, C. Fottner, S. Klose, A. Heidemeier, D. Brix, W. Fenske, S. Hahner, J. Reibetanz, B. Allolio, M. Fassnacht, G. German Adrenocortical Carcinoma Study, The role of surgery in the management of recurrent adrenocortical carcinoma, J. Clin. Endocrinol. Metab. 98 (1) (2013) 181–191, https://doi.org/10.1210/jc.2012-2559.

[15] N. Amini, G.A. Margonis, Y. Kim, T.B. Tran, L.M. Postlewait, S.K. Maithel, T. S. Wang, D.B. Evans, I. Hatzaras, R. Shenoy, J.E. Phay, K. Keplinger, R.C. Fields, L. X. Jin, S.M. Weber, A. Salem, J.K. Sicklick, S. Gad, A.C. Yopp, J.C. Mansour, Q. Y. Duh, N. Seiser, C.C. Solorzano, C.M. Kiernan, K.I. Votanopoulos, E.A. Levine, G. A. Poultsides, T.M. Pawlik, Curative Resection of Adrenocortical Carcinoma: Rates and Patterns of Postoperative Recurrence, Ann. Surg. Oncol. 23 (1) (2016) 126–133, https://doi.org/10.1245/s10434-015-4810-y.

[16] M. Terzolo, M. Fassnacht, ENDOCRINE TUMOURS: our experience with the management of patients with non-metastatic adrenocortical carcinoma, Eur. J. Endocrinol. 187 (3) (2022) R27–R40, https://doi.org/10.1530/EJE-22-0260.

[17] M. Fassnacht, M. Terzolo, B. Allolio, E. Baudin, H. Haak, A. Berruti, S. Welin, C. Schade-Brittinger, A. Lacroix, B. Jarzab, H. Sorbye, D.J. Torpy, V. Stepan, D. E. Schteingart, W. Arlt, M. Kroiss, S. Leboulleux, P. Sperone, A. Sundin, I. Hermsen, S. Hahner, H.S. Willenberg, A. Tabarin, M. Quinkler, C. de la Fouchardiere, M. Schlumberger, F. Mantero, D. Weismann, F. Beuschlein, H. Gelderblom, H. Wilmink, M. Sender, M. Edgerly, W. Kenn, T. Fojo, H.H. Muller, B. Skogseid, F.-A.S. Group, Combination chemotherapy in advanced adrenocortical carcinoma, N. Engl. J. Med 366 (23) (2012) 2189–2197, https://doi.org/10.1056/NEJMoa1200966.

[18] F. Megerle, W. Herrmann, W. Schloetelburg, C.L. Ronchi, A. Pulzer, M. Quinkler, F. Beuschlein, S. Hahner, M. Kroiss, M. Fassnacht, A.C.C.S.G. German, Mitotane monotherapy in patients with advanced adrenocortical carcinoma, J. Clin. Endocrinol. Metab. 103 (4) (2018) 1686–1695, https://doi.org/10.1210/jc.2017-02591.

[19] Y. Tang, Z. Liu, Z. Zou, J. Liang, Y. Lu, Y. Zhu, Benefits of adjuvant mitotane after resection of adrenocortical carcinoma: a systematic review and meta-analysis, Biomed. Res Int 2018 (2018) 9362108, https://doi.org/10.1155/2018/9362108.

[20] V. Chortis, A.E. Taylor, P. Schneider, J.W. Tomlinson, B.A. Hughes, D.M. O'Neil, R. Libe, B. Allolio, X. Bertagna, J. Bertherat, F. Beuschlein, M. Fassnacht, N. Karavitaki, M. Mannelli, F. Mantero, G. Opocher, E. Porfiri, M. Quinkler, M. Sherlock, M. Terzolo, P. Nightingale, C.H. Shackleton, P.M. Stewart, S. Hahner, W. Arlt, Mitotane therapy in adrenocortical cancer induces CYP3A4 and inhibits 5alpha-reductase, explaining the need for personalized glucocorticoid and androgen replacement, J. Clin. Endocrinol. Metab. 98 (1) (2013) 161–171, https://doi.org/10.1210/jc.2012-2851.

[21] M.S. Haider, T. Ahmad, J. Groll, O. Scherf-Clavel, M. Kroiss, R. Luxenhofer, The challenging pharmacokinetics of mitotane: an old drug in need of new packaging, Eur. J. Drug Metab. Pharm. 46 (5) (2021) 575–593, https://doi.org/10.1007/s13318-021-00700-5.

[22] R.B. Young, M.J. Bryson, M.L. Sweat, J.C. Street, Complexing of DDT and o,p'DDD with adrenal cytochrome P-450 hydroxylating systems, J. Steroid Biochem 4 (6) (1973) 585–591, https://doi.org/10.1016/0022-4731(73)90033-2.

[23] M. Lo Iacono, S. Puglisi, P. Perotti, L. Saba, J. Petiti, C. Giachino, G. Reimondo, M. Terzolo, Molecular mechanisms of mitotane action in adrenocortical cancer based on in vitro studies, Cancers (Basel) 13 (21) (2021), https://doi.org/10.3390/cancers13215255.

[24] C.R. Corso, A. Acco, C. Bach, S.J.R. Bonatto, B.C. de Figueiredo, L.M. de Souza, Pharmacological profile and effects of mitotane in adrenocortical carcinoma, Br. J. Clin. Pharm. 87 (7) (2021) 2698–2710, https://doi.org/10.1111/bcp.14721.

[25] S. Sbiera, E. Leich, G. Liebisch, I. Sbiera, A. Schirbel, L. Wiemer, S. Matysik, C. Eckhardt, F. Gardill, A. Gehl, S. Kendl, I. Weigand, M. Bala, C.L. Ronchi, T. Deutschbein, G. Schmitz, A. Rosenwald, B. Allolio, M. Fassnacht, M. Kroiss, Mitotane Inhibits Sterol-O-Acyl Transferase 1 Triggering Lipid-Mediated Endoplasmic Reticulum Stress and Apoptosis in Adrenocortical Carcinoma Cells, Endocrinology 156 (11) (2015) 3895–3908, https://doi.org/10.1210/en.2015-1367.

[26] S. Hescot, L. Amazit, M. Lhomme, S. Travers, A. DuBow, S. Battini, G. Boulate, I. J. Namer, A. Lombes, A. Kontush, A. Imperiale, E. Baudin, M. Lombes, Identifying mitotane-induced mitochondria-associated membranes dysfunctions: metabolomic and lipidomic approaches, Oncotarget 8 (66) (2017) 109924–109940, https://doi.org/10.18632/oncotarget.18968.

[27] S. Hescot, A. Slama, A. Lombes, A. Paci, H. Remy, S. Leboulleux, R. Chadarevian, S. Trabado, L. Amazit, J. Young, E. Baudin, M. Lombes, Mitotane alters mitochondrial respiratory chain activity by inducing cytochrome c oxidase defect in human adrenocortical cells, Endocr. Relat. Cancer 20 (3) (2013) 371–381, https://doi.org/10.1530/ERC-12-0368.

[28] A. Schiavon, L. Saba, G. Catucci, J. Petiti, S. Puglisi, C. Borin, G. Reimondo, G. Gilardi, C. Giachino, M. Terzolo, M. Lo Iacono, Albumin/mitotane interaction affects drug activity in adrenocortical carcinoma cells: smoke and mirrors on mitotane effect with possible implications for patients' management, Int J. Mol. Sci. 24 (23) (2023), https://doi.org/10.3390/ijms242316701.

[29] S. Hescot, A. Seck, M. Guerin, F. Cockenpot, T. Huby, S. Broutin, J. Young, A. Paci, E. Baudin, M. Lombes, Lipoprotein-free mitotane exerts high cytotoxic activity in adrenocortical carcinoma, J. Clin. Endocrinol. Metab. 100 (8) (2015) 2890–2898, https://doi.org/10.1210/JC.2015-2080.

[30] S. Chen, Y. Zhou, Y. Chen, J. Gu, fastp: an ultra-fast all-in-one FASTQ preprocessor, Bioinformatics 34 (17) (2018) i884–i890, https://doi.org/10.1093/bioinformatics/bty560.

[31] R. Patro, G. Duggal, M.I. Love, R.A. Irizarry, C. Kingsford, Salmon provides fast and bias-aware quantification of transcript expression, Nat. Methods 14 (4) (2017) 417–419, https://doi.org/10.1038/nmeth.4197.

[32] M.D. Robinson, D.J. McCarthy, G.K. Smyth, edgeR: a Bioconductor package for differential expression analysis of digital gene expression data, Bioinformatics 26 (1) (2010) 139–140, https://doi.org/10.1093/bioinformatics/btp616.

[33] M.E. Ritchie, B. Phipson, D. Wu, Y. Hu, C.W. Law, W. Shi, G.K. Smyth, limma powers differential expression analyses for RNA-sequencing and microarray studies, Nucleic Acids Res 43 (7) (2015) e47, https://doi.org/10.1093/nar/gkv007.

[34] M.D. Young, M.J. Wakefield, G.K. Smyth, A. Oshlack, Gene ontology analysis for RNA-seq: accounting for selection bias, Genome Biol. 11 (2) (2010) R14, https://doi.org/10.1186/gb-2010-11-2-r14.

[35] D. Wu, E. Lim, F. Vaillant, M.L. Asselin-Labat, J.E. Visvader, G.K. Smyth, ROAST: rotation gene set tests for complex microarray experiments, Bioinformatics 26 (17) (2010) 2176–2182, https://doi.org/10.1093/bioinformatics/btq401.

[36] W. Luo, C. Brouwer, Pathview: an R/Bioconductor package for pathway-based data integration and visualization, Bioinformatics 29 (14) (2013) 1830–1831, https://doi.org/10.1093/bioinformatics/btt285.

[37] C.T. Fakhry, P. Choudhary, A. Gutteridge, B. Sidders, P. Chen, D. Ziemek, K. Zarringhalam, Interpreting transcriptional changes using causal graphs: new methods and their practical utility on public networks, BMC Bioinforma. 17 (1) (2016) 318, https://doi.org/10.1186/s12859-016-1181-8.

[38] H.Y. Jiang, S.A. Wek, B.C. McGrath, D. Lu, T. Hai, H.P. Harding, X. Wang, D. Ron, D.R. Cavener, R.C. Wek, Activating transcription factor 3 is integral to the eukaryotic initiation factor 2 kinase stress response, Mol. Cell Biol. 24 (3) (2004) 1365–1377, https://doi.org/10.1128/MCB.24.3.1365-1377.2004.

[39] V. Syed, K. Mukherjee, J. Lyons-Weiler, K.M. Lau, T. Mashima, T. Tsuruo, S.M. Ho, Identification of ATF-3, caveolin-1, DLC-1, and NM23-H2 as putative antitumorigenic, progesterone-regulated genes for ovarian cancer cells by gene profiling, Oncogene 24 (10) (2005) 1774–1787, https://doi.org/10.1038/sj.onc.1207991.

[40] I.N. Mungrue, J. Pagnon, O. Kohannim, P.S. Gargalovic, A.J. Lusis, CHAC1/MGC4504 is a novel proapoptotic component of the unfolded protein response, downstream of the ATF4-ATF3-CHOP cascade, J. Immunol. 182 (1) (2009) 466–476, https://doi.org/10.4049/jimmunol.182.1.466.

[41] S. Gao, A. Ge, S. Xu, Z. You, S. Ning, Y. Zhao, D. Pang, PSAT1 is regulated by ATF4 and enhances cell proliferation via the GSK3beta/beta-catenin/cyclin D1 signaling pathway in ER-negative breast cancer, J. Exp. Clin. Cancer Res 36 (1) (2017) 179, https://doi.org/10.1186/s13046-017-0648-4.

[42] Z. Wang, M. Li, Y. Liu, Z. Qiao, T. Bai, L. Yang, B. Liu, Dihydroartemisinin triggers ferroptosis in primary liver cancer cells by promoting and unfolded protein response-induced upregulation of CHAC1 expression, Oncol. Rep. 46 (5) (2021), https://doi.org/10.3892/or.2021.8191.

[43] M.S. Chen, S.F. Wang, C.Y. Hsu, P.H. Yin, T.S. Yeh, H.C. Lee, L.M. Tseng, CHAC1 degradation of glutathione enhances cystine-starvation-induced necroptosis and ferroptosis in human triple negative breast cancer cells via the GCN2-eIF2alpha-ATF4 pathway, Oncotarget 8 (70) (2017) 114588–114602, https://doi.org/10.18632/oncotarget.23055.

[44] U. Waszut, P. Szyszka, D. Dworakowska, Understanding mitotane mode of action, J. Physiol. Pharm. 68 (1) (2017) 13–26.

[45] E. Seidel, G. Walenda, C. Messerschmidt, B. Obermayer, M. Peitzsch, P. Wallace, R. Bahethi, T. Yoo, M. Choi, P. Schrade, S. Bachmann, G. Liebisch, G. Eisenhofer, D. Beule, U.I. Scholl, Generation and characterization of a mitotane-resistant adrenocortical cell line, Endocr. Connect 9 (2) (2020) 122–134, https://doi.org/10.1530/EC-19-0510.

[46] C.W. Lin, Y.H. Chang, H.F. Pu, Mitotane exhibits dual effects on steroidogenic enzymes gene transcription under basal and cAMP-stimulating microenvironments in NCI-H295 cells, Toxicology 298 (1-3) (2012) 14–23, https://doi.org/10.1016/j.tox.2012.04.007.

[47] A. Germano, L. Saba, S. De Francia, I. Rapa, P. Perotti, A. Berruti, M. Volante, M. Terzolo, CYP11B1 has no role in mitotane action and metabolism in adrenocortical carcinoma cells, PLoS ONE [Electron. Resour.] 13 (5) (2018) e0196931.

[48] S. Hescot, A. Paci, A. Seck, A. Slama, S. Viengchareun, S. Trabado, S. Brailly-Tabard, A. Al Ghuzlan, J. Young, E. Baudin, M. Lombes, The lack of antitumor effects of o,p'DDA excludes its role as an active metabolite of mitotane for adrenocortical carcinoma treatment, Horm. Cancer 5 (5) (2014) 312–323, https://doi.org/10.1007/s12672-014-0189-7.

[49] E. Gentilin, F. Tagliati, M. Terzolo, M. Zoli, M. Lapparelli, M. Minoia, M. R. Ambrosio, E.C. Degli Uberti, M.C. Zatelli, Mitotane reduces human and mouse ACTH-secreting pituitary cell viability and function, J. Endocrinol. 218 (3) (2013) 275–285, https://doi.org/10.1530/JOE-13-0210.

[50] A.M.F. Lacombe, I.C. Soares, B.M.P. Mariani, M.Y. Nishi, J.E. Bezerra-Neto, H.D. S. Charchar, V.B. Brondani, F. Tanno, V. Srougi, J.L. Chambo, R.M. Costa de Freitas, B.B. Mendonca, A.O. Hoff, M.Q. Almeida, I. Weigand, M. Kroiss, M.C. N. Zerbini, M. Fragoso, Sterol O-Acyl Transferase 1 as a Prognostic Marker of Adrenocortical Carcinoma, Cancers (Basel) 12 (1) (2020), https://doi.org/10.3390/cancers12010247.

[51] P.M. van Koetsveld, S.G. Creemers, F. Dogan, G.J.H. Franssen, W.W. de Herder, R. A. Feelders, L.J. Hofland, The efficacy of mitotane in human primary adrenocortical carcinoma cultures, J. Clin. Endocrinol. Metab. 105 (2) (2020), https://doi.org/10.1210/clinem/dgz001.

[52] I. Weigand, B. Altieri, A.M.F. Lacombe, V. Basile, S. Kircher, L.S. Landwehr, J. Schreiner, M.C.N. Zerbini, C.L. Ronchi, F. Megerle, A. Berruti, L. Canu, M. Volante, I. Paiva, S. Della Casa, S. Sbiera, M. Fassnacht, M. Fragoso, M. Terzolo, M. Kroiss, Expression of SOAT1 in adrenocortical carcinoma and response to mitotane monotherapy: an ENSAT multicenter study, J. Clin. Endocrinol. Metab. 105 (8) (2020), https://doi.org/10.1210/clinem/dgaa293.

[53] H. Tang, R. Kang, J. Liu, D. Tang, ATF4 in cellular stress, ferroptosis, and cancer, Arch. Toxicol. 98 (4) (2024) 1025–1041, https://doi.org/10.1007/s00204-024-03681-x.

[54] A. Belavgeni, S.R. Bornstein, A. von Massenhausen, W. Tonnus, J. Stumpf, C. Meyer, E. Othmar, M. Latk, W. Kanczkowski, M. Kroiss, C. Hantel, C. Hugo, M. Fassnacht, C.G. Ziegler, A.V. Schally, N.P. Krone, A. Linkermann, Exquisite sensitivity of adrenocortical carcinomas to induction of ferroptosis, Proc. Natl. Acad. Sci. USA 116 (44) (2019) 22269–22274, https://doi.org/10.1073/pnas.1912700116.

[55] I. Weigand, J. Schreiner, F. Rohrig, N. Sun, L.S. Landwehr, H. Urlaub, S. Kendl, K. Kiseljak-Vassiliades, M.E. Wierman, J.P.F. Angeli, A. Walch, S. Sbiera, M. Fassnacht, M. Kroiss, Active steroid hormone synthesis renders adrenocortical cells highly susceptible to type II ferroptosis induction, Cell Death Dis. 11 (3) (2020) 192, https://doi.org/10.1038/s41419-020-2385-4.